

Electronic Supplementary Information

Calcium-induced reversible assembly of phosphorylated amphiphile within lipid bilayer membranes

Yusuke Shimizu,^a Kohei Sato,^{*a} and Kazushi Kinbara^{*a,b}

^a School of Life Science and Technology, Tokyo Institute of Technology,

4259 Nagatsuta-cho, Midori-ku, Yokohama, Kanagawa, 226-8501 Japan

^b World Research Hub Initiative, Institute of Innovative Research, Tokyo Institute of

Technology, 4259 Nagatsuta-cho, Midori-ku, Yokohama 226-8501, Japan

Table of Contents

1.	General	S3
2.	Synthesis	
	2.1. Synthesis of 3	S4
	2.2. Synthesis of 4	S4
	2.3. Synthesis of PA	S5
3.	Analytical data	
	3.1. ¹ H, ¹³ C, and ³¹ P NMR spectroscopy	S6
	3.2. High resolution ESI-TOF mass spectrometry	S10
4.	Methods	
	4.1. Preparation of giant unilamellar vesicles (GUVs) for microscopy	S12
	4.2. Preparation of large unilamellar vesicles (LUVs) for spectroscopy.....	S12
	4.3. Preparation of LUVs for fluorescence depth quenching	S12
	4.4. Acid-base titration of PA	S13

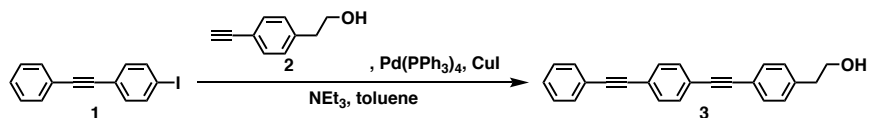
5.	Supplementary data	
5.1.	Emission spectra of PA	S14
5.2.	Dynamic light scattering of PA in HEPES buffer	S14
5.3.	Dynamic light scattering of PA -containing LUVs	S15
5.4.	Fluorescence depth quenching of PA -containing LUVs	S15
5.5.	Emission spectra of PA -containing LUVs upon addition of CaCl ₂	S16
5.6.	Acid-base titration of PA	S16
5.7.	Emission spectra of PA -containing LUVs upon sequential addition of CaCl ₂ and EDTA	S17
5.8.	Optical micrographs of PA -containing GUVs upon sequential addition of CaCl ₂ and EDTA.....	S18
5.9.	Dynamic light scattering of PA -containing LUVs upon sequential addition of CaCl ₂ and EDTA.....	S19
6.	References	S20

1. General

Unless otherwise noted, all commercial reagents were used as received. Gradient flash silica column chromatography was performed on a Biotage model Isolera One. ^1H , ^{13}C , and ^{31}P NMR spectra were recorded on a Bruker model biospin AVANCE III 500 spectrometer, operating at 500, 125, and 202 MHz for ^1H , ^{13}C , and ^{31}P NMR, respectively, where chemical shifts were determined with respect to tetramethylsilane or a residual non-deuterated solvent as internal references, and phosphoric acid as an external reference. Electrospray ionization time-of-flight (ESI-TOF) mass spectrometry was performed on a Bruker model micrOTOF II. Electronic absorption spectra were recorded on a JASCO model V-650 UV-Vis spectrophotometer using a quartz cell of 10 mm optical path length. Fluorescent spectra were recorded on a JASCO model FP-6500 spectrofluorometer using a quartz cell of 10 mm optical path length. Dynamic light scattering (DLS) was performed on a Malvern model Zetasizer Nano ZSP spectrophotometer using a quartz cell of 10 mm optical path length. Fluorescence and phase contrast microscopic observations were performed on a Olympus model IX-71 microscope, where a U-MWU2 mirror unit (excitation filter: 330–385 nm, emission filter: 420 nm, dichroic mirror: 400 nm) was used for fluorescence imaging. A 0.1 mm thick silicon-based spacer was placed between a slide glass and a coverslip for imaging. Acid-base titration was performed on a HORIBA model LAQUA F-72 desktop pH meter equipped with a 9618S-10D micro ToupH electrode.

2. Synthesis

2.1. Synthesis of 3



To a dry triethylamine/toluene solution (1.3 mL and 0.75 mL, respectively) of compound **1**^{S1} (172 mg, 566 μmol) and compound **2**^{S2} (92.5 mg, 633 μmol), after being degassed by three freeze-pump-thaw cycling, were added tetrakis(triphenylphosphine) palladium(0) (30.6 mg, 26.5 μmol) and copper(I) iodide (7.7 mg, 40.4 μmol) under Ar at room temperature, and the resultant mixture was stirred overnight at the same temperature. The resultant precipitate was filtered and washed with hexane, and the collected solid was suspended in methanol and filtered off from insoluble substances through a filter paper. The filtrate was evaporated to dryness under reduced pressure, and the resultant solid was washed with cold chloroform to afford compound **3** as a white solid (128 mg, 397 μmol , 70%). ¹H NMR (500 MHz, CDCl₃, 25 °C, ppm): δ 7.55–7.48 (m, 8H), 7.37–7.35 (m, 3H), 7.24 (d, J = 8.2 Hz, 2H), 3.89 (q, J = 6.2 Hz, 2H), 2.90 (t, J = 6.6 Hz, 2H), 1.40 (t, J = 5.8 Hz, 1H); ¹³C NMR (125 MHz, CDCl₃, 25 °C, ppm): δ 139.40, 132.05, 131.85, 131.74, 131.72, 129.35, 128.68, 128.61, 123.38, 123.26, 121.42, 91.42, 91.35, 89.33, 89.18, 63.66, 39.35; HRMS (ESI-TOF-MS) m/z calculated for C₂₄H₁₈ONa [M + Na]⁺: 345.1255, found: 345.1233.

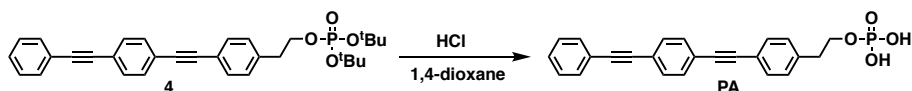
2.2. Synthesis of 4



To a dry DMF solution of compound **3** (100 mg, 310 μmol), imidazole (20.8 mg, 306 μmol) and imidazole hydrochloride^{S3} (53.0 mg, 507 μmol) was added di-*tert*-butyl *N,N*-diisopropylphosphoramidite (356 mg, 400 μL , 1.3 mmol) dropwise over 3 min under Ar at room temperature, and the resultant mixture was stirred for 7 hours at the same temperature. The reaction mixture was cooled to 0 °C, and 30 wt% hydrogen peroxide (250 μL) was added dropwise and stirred for 3 hours at room temperature. Then, the reaction mixture was diluted with ethyl acetate and the organic phase was washed three

times with water and once with brine, dried over Na₂SO₄, and evaporated to dryness under reduced pressure. The residue was purified by gradient flash silica column chromatography using a SNAP KP-Sil 50 g cartridge with hexane and ethyl acetate (93/7 to 40/60) as eluents, followed by size exclusion chromatography using CHCl₃ as an eluent to allow isolation of compound **4** as a white solid (76.0 mg, 148 μmol, 48%). ¹H NMR (500 MHz, CDCl₃, 25 °C, ppm): δ 7.54–7.52 (m, 2H), 7.50 (s, 4H), 7.47 (d, *J* = 8.2 Hz, 2H), 7.37–7.34 (m, 3H), 7.23 (d, *J* = 8.2 Hz, 2H), 4.16 (q, *J* = 6.9 Hz, 2H), 2.99 (t, *J* = 6.9 Hz, 2H), 1.87 (s, 1H), 1.44 (s, 18H); ¹³C NMR (125 MHz, CDCl₃, 25 °C, ppm): δ 138.59, 131.87, 131.80, 131.70, 131.68, 129.35, 128.64, 128.57, 123.40, 123.21, 121.39, 91.39, 89.30, 89.10, 82.49, 82.43, 67.07 (d, *J* = 6.4 Hz), 36.86 (d, *J* = 7.8 Hz), 30.01 (d, *J* = 4.1 Hz); ³¹P NMR (202 MHz, CDCl₃, 25 °C, ppm): δ –10.91; HRMS (ESI-TOF-MS) *m/z* calculated for C₃₂H₃₅O₄PNa [M + Na]⁺: 537.2171, found: 537.2147.

2.3. Synthesis of PA



A 1,4-dioxane solution of HCl (4 M, 800 μL, 3.2 mmol) was added to compound **4** (51.4 mg, 99.9 μmmol) at room temperature under Ar, and the resultant mixture was stirred for 5 hours at the same temperature. Then, the reaction mixture was evaporated to dryness under reduced pressure to afford **PA** as a white solid (42.5 mg, 98.1 μmol, 98%, containing 2wt% of 1,4-dioxane). ¹H NMR (500 MHz, DMSO-*d*₆, 25 °C, ppm): δ 7.60–7.57 (m, 6H), 7.53–7.52 (d, *J* = 7.7 Hz, 2H), 7.46–7.44 (m, 2H), 4.05 (q, *J* = 6.7 Hz, 2H), 2.94 (t, *J* = 6.7 Hz, 2H); ¹³C NMR (125 MHz, DMSO-*d*₆, 25 °C, ppm): δ 139.53, 131.68, 131.64, 131.45, 131.41, 129.40, 129.07, 128.82, 122.61, 122.34, 122.00, 119.91, 91.51, 91.35, 88.90, 88.60, 65.39 (d, *J* = 5.1 Hz), 35.99 (d, *J* = 6.8 Hz); ³¹P NMR (202 MHz, DMSO-*d*₆, 25 °C, ppm): δ 0.74; HRMS (ESI-TOF-MS) *m/z* calculated for C₂₄H₁₈O₄P [M]⁻: 401.0948, found: 401.0937.

3. Analytical data

3.1. ^1H , ^{13}C , and ^{31}P NMR spectroscopy

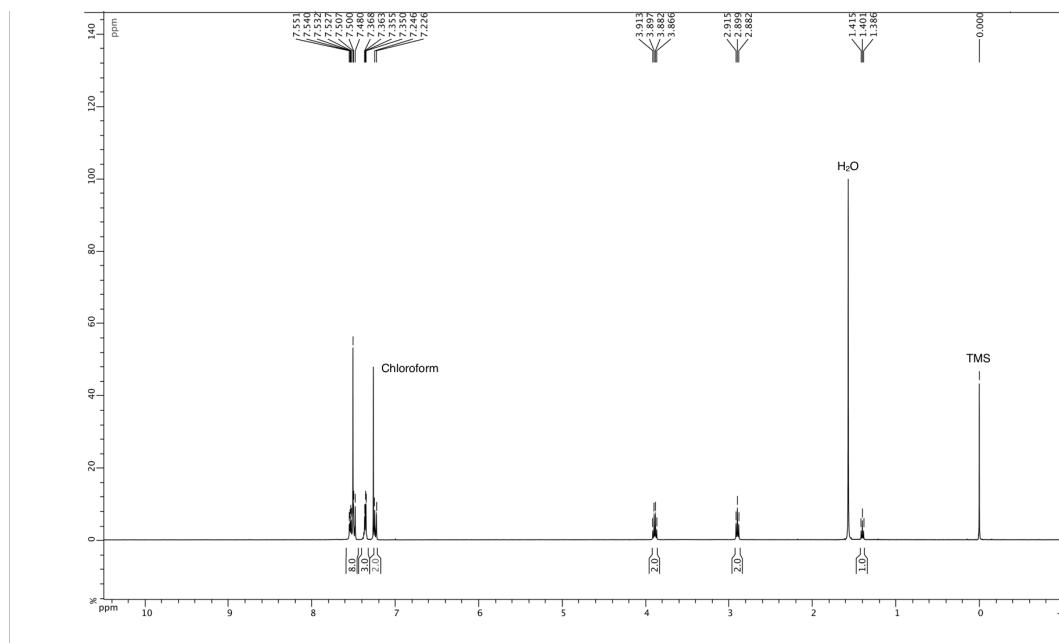


Fig. S1. ^1H NMR spectrum (500 MHz) of **3** in CDCl_3 at 25 °C.

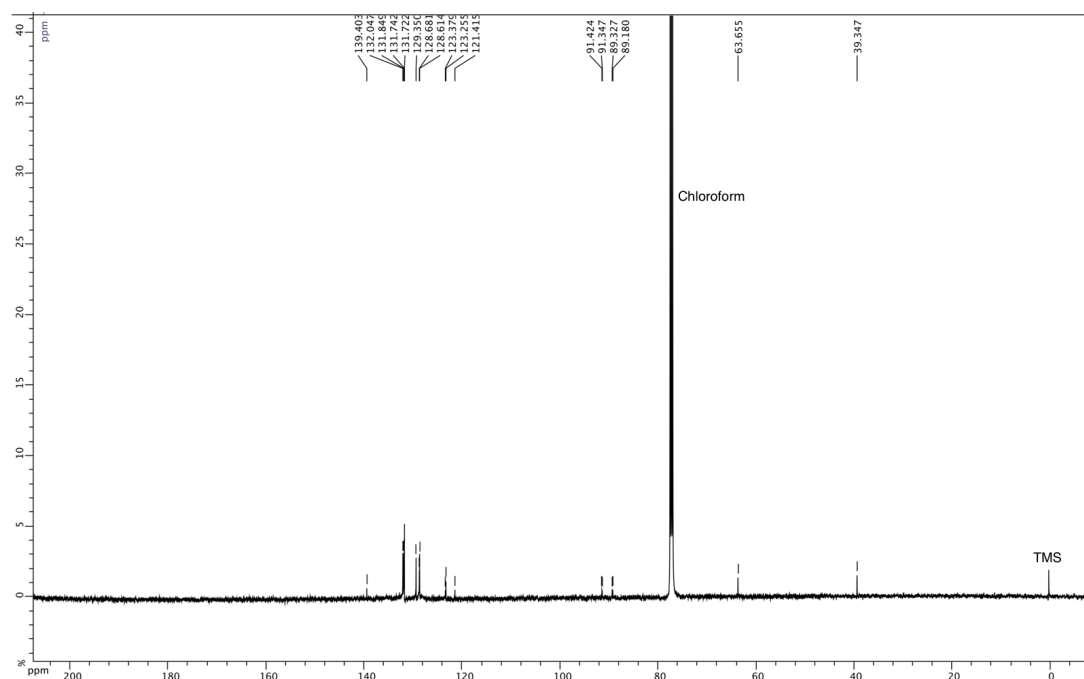


Fig. S2. ^{13}C NMR spectrum (125 MHz) of **3** in CDCl_3 at 25 °C.

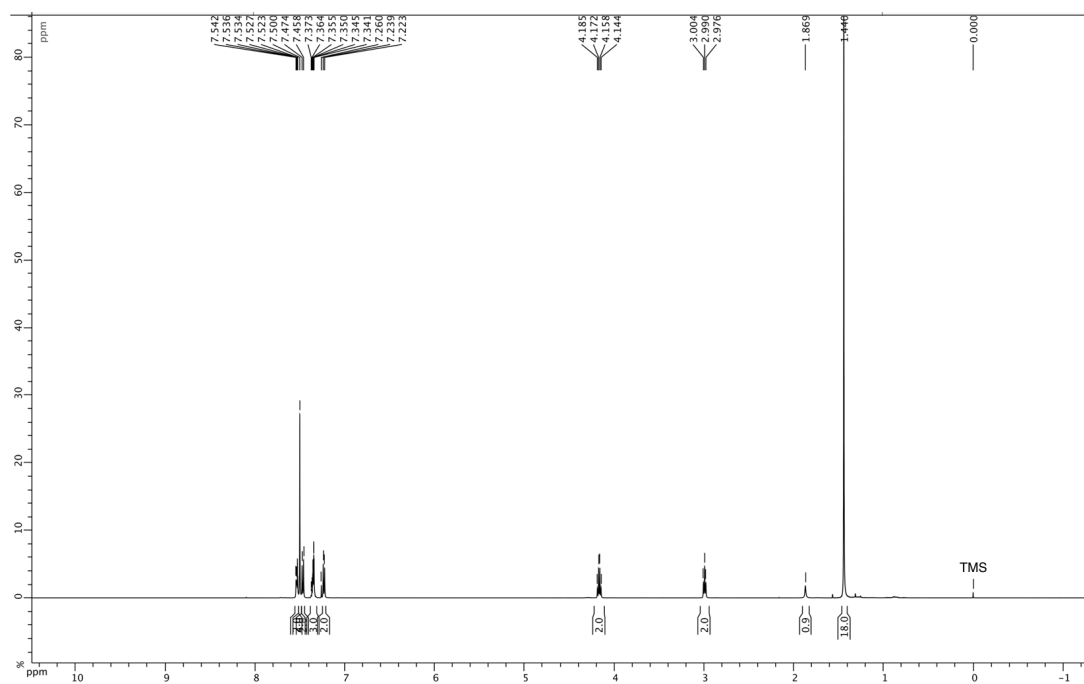


Fig. S3. ^1H NMR spectrum (500 MHz) of **4** in CDCl_3 at 25 °C.

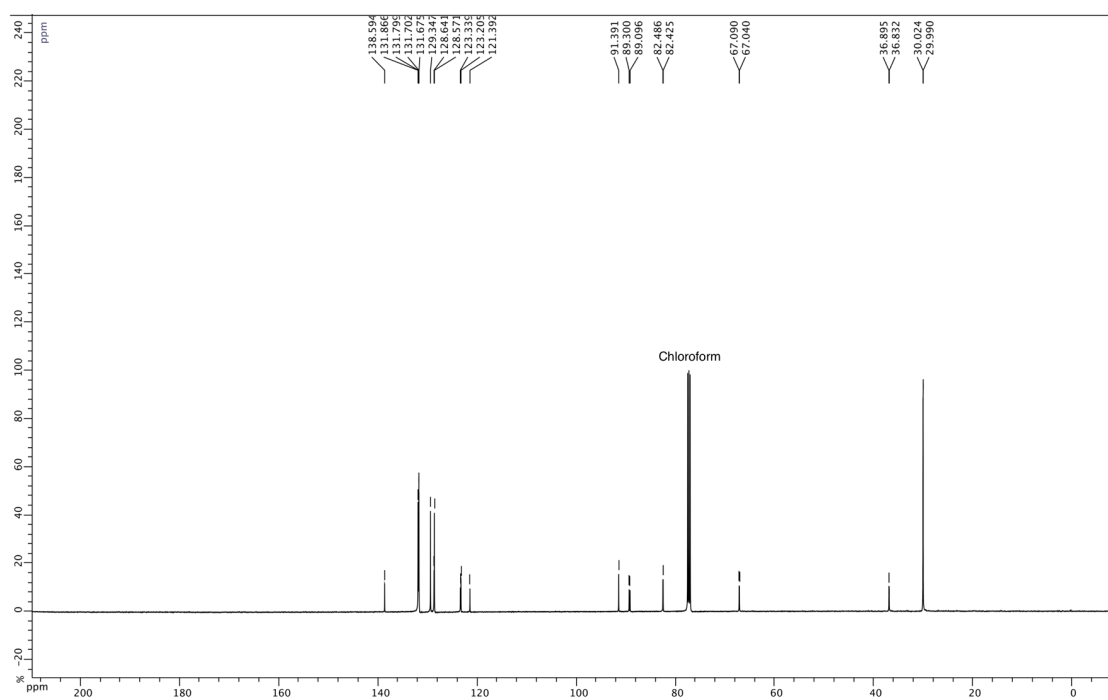


Fig. S4. ^{13}C NMR spectrum (125 MHz) of **4** in CDCl_3 at 25 °C.

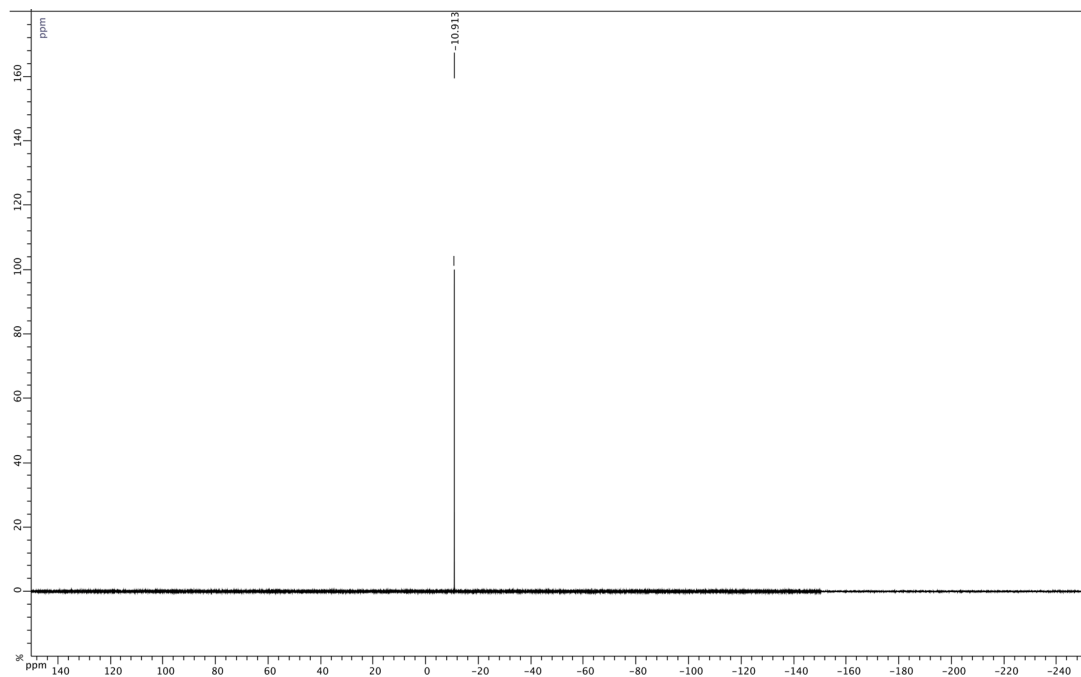


Fig. S5. ^{31}P NMR spectrum (202 MHz) of **4** in CDCl_3 at 25 °C.

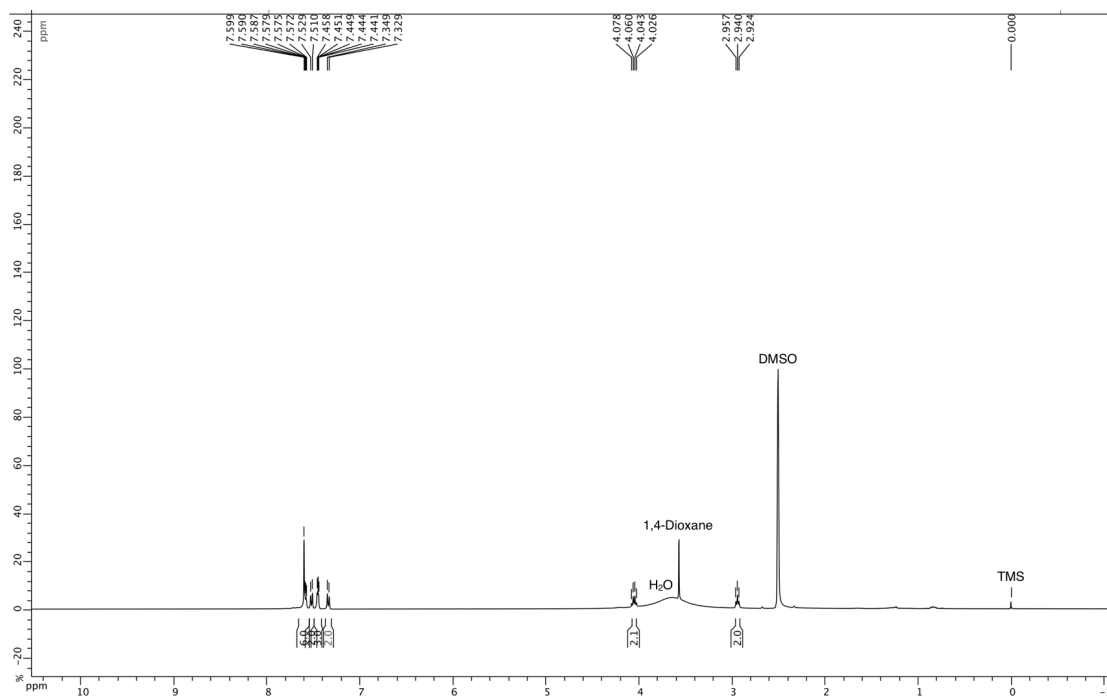


Fig. S6. ^1H NMR spectrum (500 MHz) of **PA** in $\text{DMSO}-d_6$ at 25 °C.

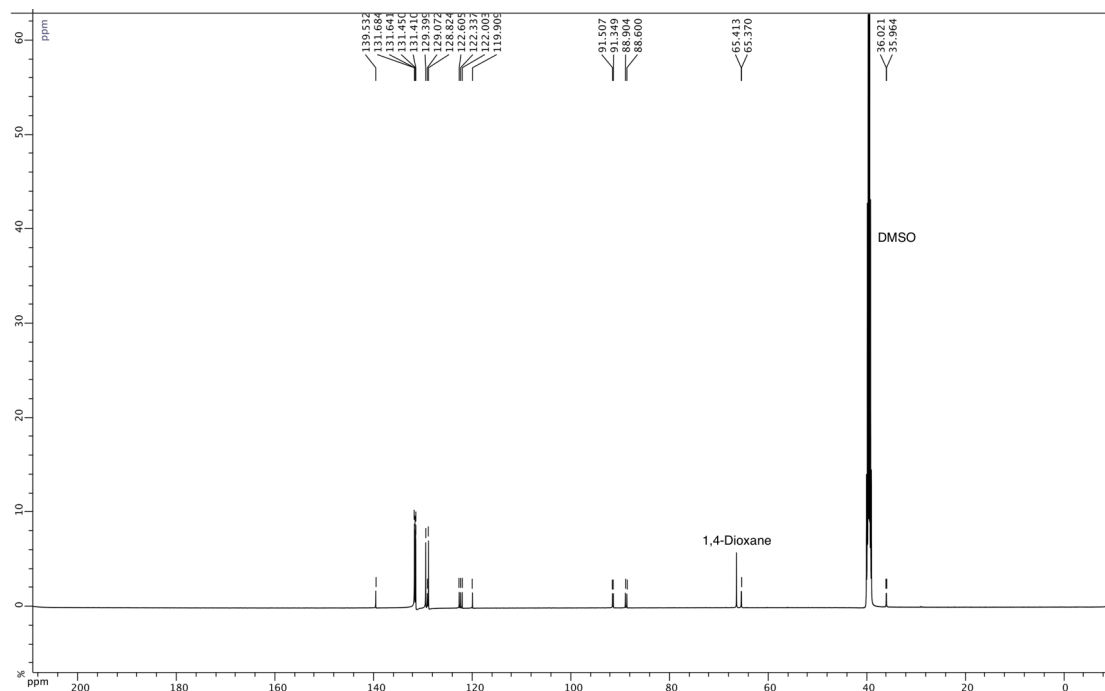


Fig. S7. ^{13}C NMR spectrum (125 MHz) of PA in $\text{DMSO-}d_6$ at 25 °C.

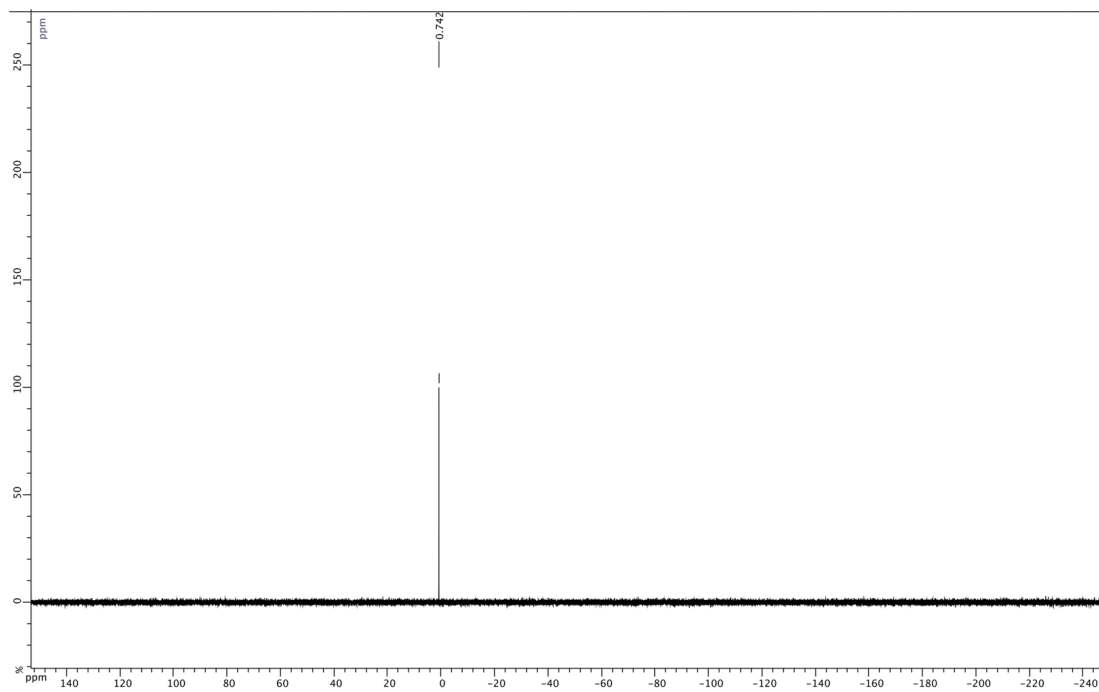


Fig. S8. ^{31}P NMR spectrum (202 MHz) of PA in $\text{DMSO-}d_6$ at 25 °C.

3.2. High-resolution ESI-TOF mass spectrometry

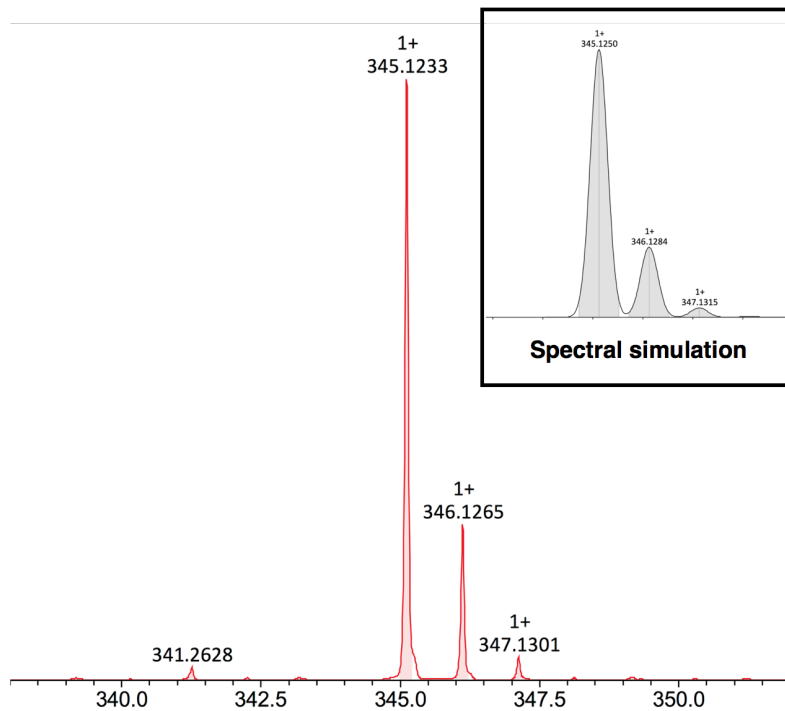


Fig. S9. High-resolution ESI-TOF mass spectrum of **3**.

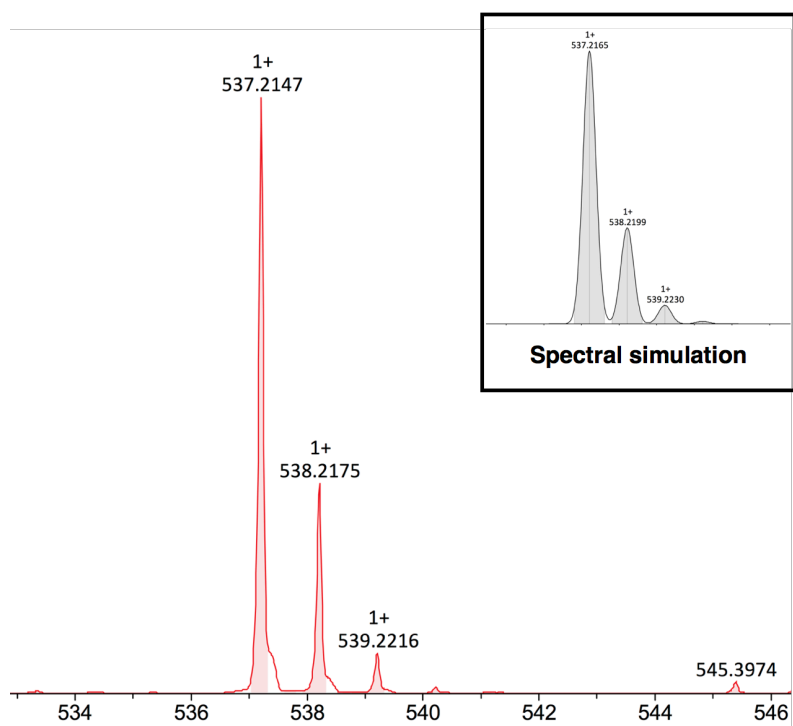


Fig. S10. High-resolution ESI-TOF mass spectrum of **4**.

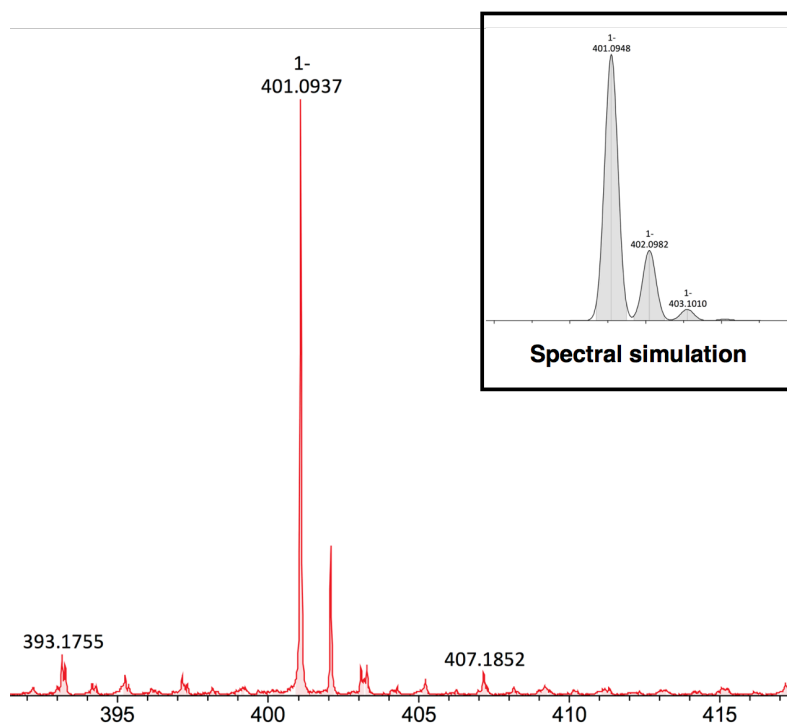


Fig. S11. High-resolution ESI-TOF mass spectrum of PA.

4. Methods

4.1. Preparation of giant unilamellar vesicles (GUVs) for microscopy

To a CHCl_3 solution (100 μL) of 1,2-dioleoyl-*sn*-glycero-3-phosphocholine (DOPC) ([DOPC] = 6.0 mM) was added a DMSO solution (3 μL) of PA ([PA] = 9.8 mM). The resultant mixture was slowly deposited and dried on indium tin oxide (ITO)-coated glass slide at room temperature, and the resulting film was further dried under high vacuum at the same temperature overnight. A lipid film developed on the surface of ITO-coated slide glass was sandwiched using another ITO-coated glass slide with a 0.1 mm thick silicon-based spacer, and the film was hydrated with aqueous sucrose ([sucrose] = 200 μM , 300 μL). Then, an AC voltage with an amplitude of 1.4 V and frequency of 10 Hz was applied to the electrode at room temperature for 2 hours to afford a dispersion of DOPC GUVs containing PA ([DOPC] = 2.0 mM, [PA] = 98 μM). The dispersion (10 μL) was diluted with aqueous sucrose ([sucrose] = 200 μM , 90 μL) before microscopic observations.

4.2. Preparation of large unilamellar vesicles (LUVs) for absorption and emission spectroscopy

To a CHCl_3 solution (1.2 mL) of DOPC ([DOPC] = 5.0 mM) was added a DMSO solution (30 μL) of PA ([PA] = 9.8 mM), and the resultant mixture was slowly evaporated to dryness in a test tube at room temperature. The resultant film was further dried under high vacuum at the same temperature overnight. A lipid film developed on the inner surface of the test tube was hydrated with a HEPES buffer ([HEPES] = 20 mM, [NaCl] = 50 mM, pH 7.0, 600 μL) at 37 °C for 1 hour, and the resultant suspension was vortexed at room temperature for 1 min. After 5 freeze-to-thaw cycles, the resultant dispersion was extruded through a porous polycarbonate membrane with a pore diameter of 100 nm for 21 times at room temperature to afford a dispersion of DOPC LUVs containing PA ([DOPC] = 10 mM, [PA] = 490 μM). The dispersion (60 μL) was diluted with HEPES buffer ([HEPES] = 20 mM, [NaCl] = 50 mM, pH 7.0, 2940 μL) before spectroscopic measurements.

4.3. Preparation of LUVs for fluorescence depth quenching

To a CHCl_3 solution (672 μL) of phosphocholine (PC) ([total PC] = 3.6 mM ([DOPC]/[X-doxyl-PC] = 9/1, X = 5, 12, or 16) was added a DMSO solution (12 μL) of PA ([PA] =

9.8 mM), and the resultant mixture was slowly evaporated to dryness in a test tube at room temperature. The resultant film was further dried under high vacuum at the same temperature overnight. A lipid film developed on the inner surface of the test tube was hydrated with a HEPES buffer ([HEPES] = 20 mM, [NaCl] = 50 mM, pH 7.0, 960 μ L) at 37 °C for 1 hour, and the resultant suspension was vortexed at room temperature for 1 min. After 5 freeze-to-thaw cycles, the resultant dispersion was extruded through a porous polycarbonate membrane with a pore diameter of 100 nm for 21 times at room temperature to afford a dispersion of **PA**-containing LUVs ([total PC] = 2.5 mM ([DOPC]/[X-doxyl-PC] = 9/1, X = 5, 12, or 16), [**PA**] = 123 μ M). The dispersion (240 μ L) was diluted with HEPES buffer ([HEPES] = 20 mM, [NaCl] = 50 mM, pH 7.0, 2760 μ L) before spectroscopic measurements.

4.4. Acid-base titration for determination of pK_a

To a DMSO solution (128 μ L) of **PA** ([**PA**] = 98 mM) was added filtered deionized H₂O (1092 μ L) and aqueous NaOH ([NaOH] = 1.0 M, 60 μ L), and the resultant solution was titrated by aqueous HCl ([HCl] = 1.0 M). The pH changes were monitored using a pH meter.

5. Supplementary data

5.1. Emission spectra of PA

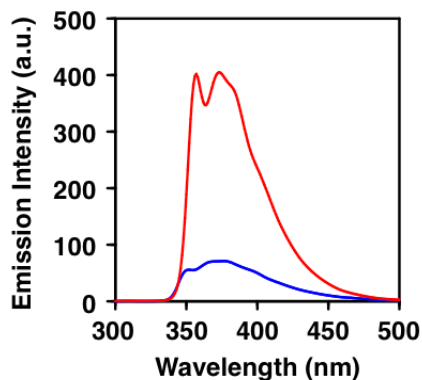


Fig. S12. Emission spectra of PA ($[PA] = 9.8 \mu\text{M}$) in DMSO (red) and in HEPES buffer ($[HEPES] = 20 \text{ mM}$, $[NaCl] = 50 \text{ mM}$, pH 7.0, containing 0.1% (v/v) DMSO) (blue) at $37 \text{ }^\circ\text{C}$ ($\lambda_{\text{ex}} = 280 \text{ nm}$).

5.2. Dynamic light scattering of PA in HEPES buffer

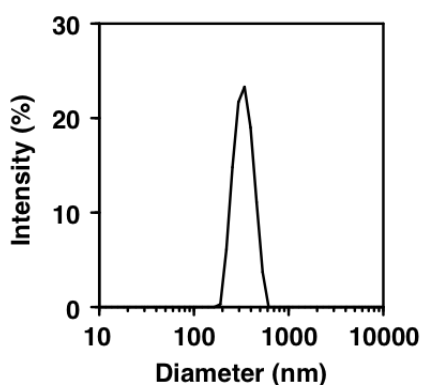


Fig. S13. Intensity-based particle-size distribution profiles of PA ($[PA] = 9.8 \mu\text{M}$) in HEPES buffer ($[HEPES] = 20 \text{ mM}$, $[NaCl] = 50 \text{ mM}$, pH 7.0) at $37 \text{ }^\circ\text{C}$, analyzed by dynamic light scattering. Mean hydrodynamic diameter of the particles: 328.7 nm.

5.3. Dynamic light scattering of PA-containing LUVs

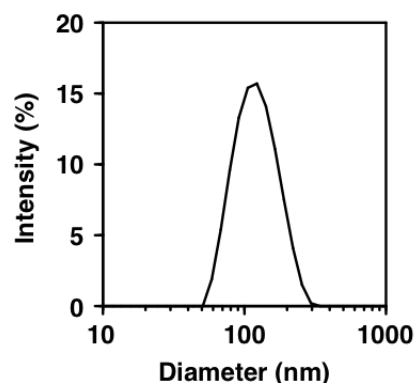


Fig. S14. Intensity-based particle-size distribution profiles of **PA**-containing LUVs ([DOPC] = 200 μ M, [**PA**] = 9.8 μ M) in HEPES buffer ([HEPES] = 20 mM, [NaCl] = 50 mM, pH 7.0) at 37 $^{\circ}$ C, analyzed by dynamic light scattering. Mean hydrodynamic diameter of the particles: 113.1 nm.

5.4. Fluorescence depth quenching of PA-containing LUVs

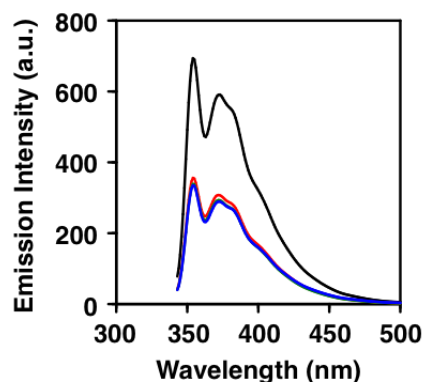


Fig. S15. Emission spectra of **PA**-containing LUVs ([total PC] = 200 μ M ([DOPC]/[X-doxy PC] = 9/1), [**PA**] = 9.8 μ M) in HEPES buffer ([HEPES] = 20 mM, [NaCl] = 50 mM, pH 7.0) at 37 $^{\circ}$ C (λ_{ex} = 323 nm). The PCs used for LUVs were DOPC (black), and mixtures of DOPC with 5-doxy PC (red), 12-doxy PC (green), or 16-doxy PC (blue).

5.5. Emission spectra of PA-containing LUVs upon addition of CaCl₂

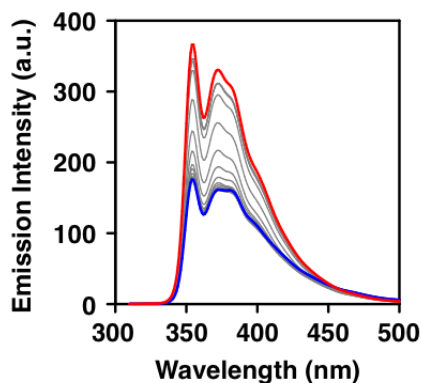


Fig. S16. Emission spectra of **PA**-containing LUVs ($[\text{DOPC}] = 200 \mu\text{M}$, $[\text{PA}] = 9.8 \mu\text{M}$) in HEPES buffer ($[\text{HEPES}] = 20 \text{ mM}$, $[\text{NaCl}] = 50 \text{ mM}$, pH 7.0) upon addition of CaCl_2 ($0 \mu\text{M}$ (red), $1.0 \mu\text{M}$, $2.5 \mu\text{M}$, $5 \mu\text{M}$, $10 \mu\text{M}$, $25 \mu\text{M}$, $50 \mu\text{M}$, $100 \mu\text{M}$, $250 \mu\text{M}$, $500 \mu\text{M}$, 1.0 mM , 2.5 mM , 5.0 mM , 10 mM , and 25 mM (blue)) at $37 \text{ }^\circ\text{C}$ ($\lambda_{\text{ex}} = 290 \text{ nm}$).

5.6. Acid-base titration of PA

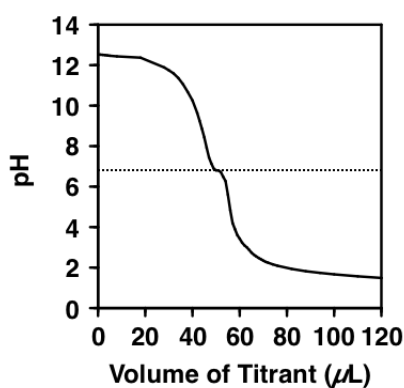


Fig. S17. Acid-base titration curve of **PA** in aqueous NaOH ($[\text{PA}] = 9.8 \text{ mM}$, $[\text{NaOH}] = 46.9 \text{ mM}$) upon addition of aqueous HCl ($[\text{HCl}] = 1.0 \text{ M}$) at $25 \text{ }^\circ\text{C}$.

Based on the titration curve, $\text{p}K_{\text{a}1}$ was evaluated to be 6.8, however, $\text{p}K_{\text{a}2}$ could not be evaluated because **PA** started to form precipitates below pH 2.0. Previous studies on phosphate monoesters indicate that $\text{p}K_{\text{a}2}$ is below 2.0,^{S4} thus **PA** is most likely negatively charged under pH 7.0.

5.7. Emission spectra of PA-containing LUVs upon sequential addition of CaCl₂ and EDTA

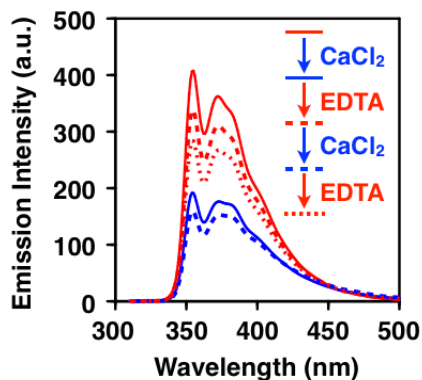


Fig. S18. Emission spectra of PA-containing LUVs ([DOPC] = 200 μ M, [PA] = 9.8 μ M) in HEPES buffer ([HEPES] = 20 mM, [NaCl] = 50 mM, pH 7.0) before (red solid curve) and after sequential addition of (i) CaCl₂ ([CaCl₂] = 1.0 mM) (blue solid curve), (ii) EDTA ([EDTA] = 1.1 mM) (red broken curve), (iii) CaCl₂ ([CaCl₂] = 1.2 mM) (blue broken curve), and (iv) EDTA ([EDTA] = 1.3 mM) (red dotted curve) at 37 °C (λ_{ex} = 290 nm).

5.8. Optical micrographs of PA-containing GUVs upon sequential addition of CaCl₂ and EDTA

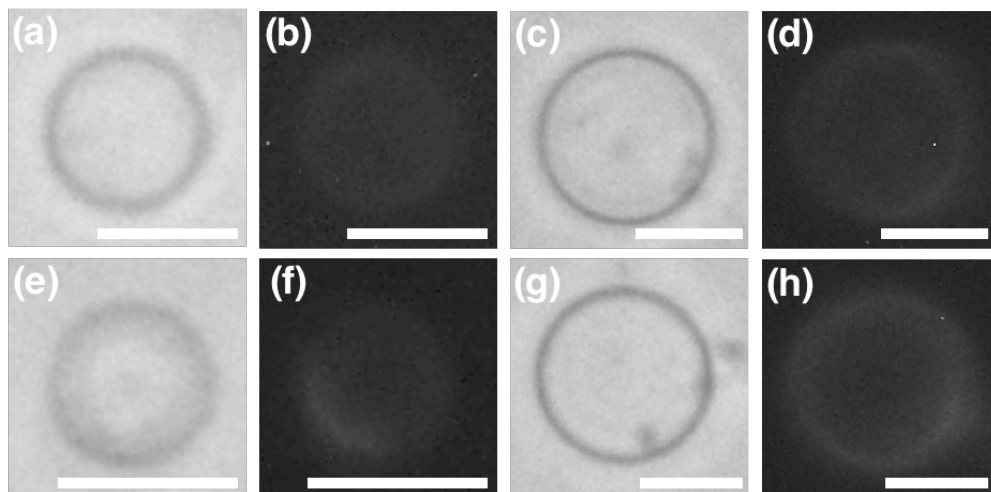


Fig. S19. (a, c, e, g) Phase-contrast and (b, d, f, h) fluorescence micrographs ($\lambda_{\text{ex}} = 330\text{--}385\text{ nm}$, $\lambda_{\text{obsd}} > 420\text{ nm}$) of PA-containing GUVs upon sequential addition of CaCl₂ and EDTA in aqueous sucrose ([sucrose] = 200 μM) at 25 °C. (a, b) After the addition of CaCl₂ ([CaCl₂] = 1.0 mM), (c,d) followed by the addition of EDTA ([EDTA] = 1.1 mM), (e, f) CaCl₂ ([CaCl₂] = 1.2 mM), and (g, h) EDTA ([EDTA] = 1.3 mM). Scale bars: 10 μm .

5.9. Dynamic light scattering of PA-containing LUVs upon sequential addition of CaCl₂ and EDTA

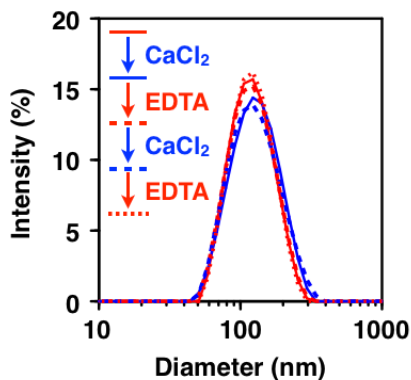


Fig. S20. Intensity-based particle-size distribution profiles of PA-containing LUVs ([DOPC] = 200 μ M, [PA] = 9.8 μ M) in HEPES buffer ([HEPES] = 20 mM, [NaCl] = 50 mM, pH 7.0) (i) before (red solid curve) and after sequential addition of (ii) CaCl₂ ([CaCl₂] = 1.0 mM) (blue solid curve), (iii) EDTA ([EDTA] = 1.1 mM) (red broken curve), (iv) CaCl₂ ([CaCl₂] = 1.2 mM) (blue broken curve), and (v) EDTA ([EDTA] = 1.3 mM) (red dotted curve) at 37 °C, analyzed by dynamic light scatterings. Mean hydrodynamic diameters of the particles: (i) 113.1 nm, (ii) 116.6 nm, (iii) 111.9 nm, (iv) 115.8 nm, (v) 112.8 nm.

6. References

- (S1) K. Semba, T. Fujihara, T. Xu, J. Terao and Y. Tsuji, *Adv. Synth. Catal.*, 2012, **354**, 1542–1550.
- (S2) A. Ouach, F. Pin, E. Bertrand, J. Vercouillie, Z. Gulhan, C. Mothes, J.-B. Deloye, D. Guilloteau, F. Suzenet, S. Chalon and S. Routier, *Eur. J. Med. Chem.*, 2016, **107**, 153–164.
- (S3) T. Peppel, C. Roth, K. Fumino, D. Paschek, M. Köckerling and R. Ludwig, *Angew. Chem., Int. Ed.*, 2011, **50**, 6661–6665.
- (S4) W. D. Kumler and J. J. Eiler, *J. Am. Chem. Soc.*, 1943, **65**, 2355–2361.